ACS APPLIED MATERIALS & INTERFACES

Research Article

www.acsami.org

"Turn-on" Fluorescence Detection of Lead Ions Based on Accelerated Leaching of Gold Nanoparticles on the Surface of Graphene

Xiuli Fu,[†,‡,§] Tingting Lou,[†,‡,§] Zhaopeng Chen,[†,‡] Meng Lin,[†,‡] Weiwei Feng,[†,‡] and Lingxin Chen*[,†,‡]

[†]Key Laboratory of Coastal Zone Environmental Processes, Yantai Institute of Coastal Zone Research, Chinese Academy of Sciences, Yantai 264003, China

[‡]Shandong Provincial Key Laboratory of Coastal Zone Environmental Processes, Yantai Institute of Coastal Zone Research, Yantai 264003, China

[§]Graduate University of Chinese Academy of Sciences, Beijing 100049, China

ABSTRACT: A novel platform for effective "turn-on" fluorescence sensing of lead ions (Pb^{2+}) in aqueous solution was developed based on gold nanoparticle (AuNP)-functionalized graphene. The AuNP-functionalized graphene exhibited minimal background fluorescence because of the extraordinarily high quenching ability of AuNPs. Interestingly, the AuNP-functionalized graphene underwent fluorescence restoration as well as significant enhancement upon adding Pb^{2+}, which was attributed to the fact that Pb^{2+} could accelerate the leaching rate of the AuNPs on graphene surfaces in the presence of both thiosulfate ($S_2O_3^{2-}$) and 2-mercaptoethanol (2-ME). Consequently, this could be utilized as the basis for selective detection of Pb^{2+}. With the optimum conditions chosen, the relative fluorescence intensity showed good linearity versus logarithm concentration of Pb^{2+} in the range of 50−1000 nM (R = 0.9982), and a detection limit of 10 nM. High selectivity over common coexistent metal ions was also demonstrated. The practical application had been carried out for determination of Pb^{2+} in tap water and mineral water samples. The Pb^{2+}-specific "turn-on" fluorescence sensor, based on Pb^{2+} accelerated leaching of AuNPs on the surface of graphene, provided new opportunities for highly sensitive and selective Pb^{2+} detection in aqueous media.

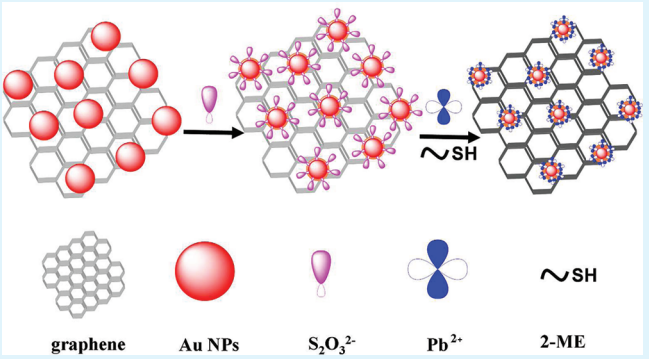

KEYWORDS: *lead ions, fluorescence detection, graphene, gold nanoparticles, leaching*

INTRODUCTION

Graphene, a monolayer of carbon atoms packed into a honeycomb two-dimensional crystal structure, has attracted intensive interests in recent years, due to its remarkable electronic, mechanical, optical and thermal properties.[1−4] Particularly, graphene has found important applications in fluorescence detection.[5−8] In addition to the ability of quenching fluorescence, both graphene and graphene oxide (GO) have the characteristic of photoluminescence arising from electron−hole pairs localized within small sp^2 carbon clusters embedded in a sp^3 matrix.[9−11] Seo and co-workers had demonstrated that GO photoluminescence could be quenched by gold nanoparticles (AuNPs) because of fluorescence resonance energy transfer (FRET) between GO and AuNPs.[12,13] However, there are still few studies about graphene photoluminescence based on "turn-on" FRET.

Recently, graphene-metal nanocomposites have been synthesized in a water-ethylene glycol mixture system.[14,15] The nanocomposites possess particular properties applicable in certain technology fields such as optical, electrical and sensor areas.[16] For the graphene-gold nanocomposites (G-Au NCs), the AuNPs on the surface of graphene can not only enhance the Raman intensity but also quench the graphene fluorescence.[15] AuNPs have been proved to be excellent quenchers of fluorophores such as organic fluorescent tags[17] and semiconductor fluorescent quantum dots.[18] Once the AuNPs are leached from the surface of graphene, especially they are completely dissolved into the solution, the fluorescence of graphene can greatly recover and increase, with "turn-on" fluorescence observed.

According to the previous researches, AuNPs could be leached in the ammoniacal thiosulfate ($S_2O_3^{2-}$) system, and the important parameters influencing the dissolution behavior of gold in the ammoniacal $S_2O_3^{2-}$ system have been investigated.[19−24] Also, these studies have suggested that some heavy metals, such as Pb, Ag, and Hg, could enhance gold leaching. Notably, Huang and co-workers have developed a sensitive method based on the fact that Pb^{2+} ions could accelerate the leaching rate of AuNPs by both $S_2O_3^{2-}$ and 2-mercaptoethanol, for colorimetric assay of Pb^{2+}.[25]

Meanwhile, as is well-known, heavy metal pollution, as a severe environmental problem, has received increasing

Received: December 5, 2011
Accepted: January 20, 2012
Published: January 20, 2012

   dx.doi.org/10.1021/am201711j | *ACS Appl. Mater. Interfaces* 2012, 4, 1080−1086

Scheme 1. Schematic Representation of the Sensing Mechanism for the Detection of Pb^{2+} Ions Based on Accelerated Leaching of Gold Nanoparticles on the Surface of Graphene

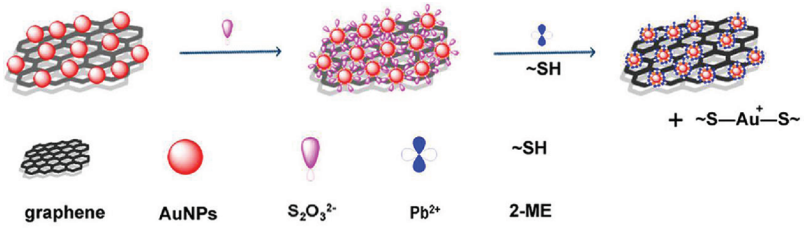

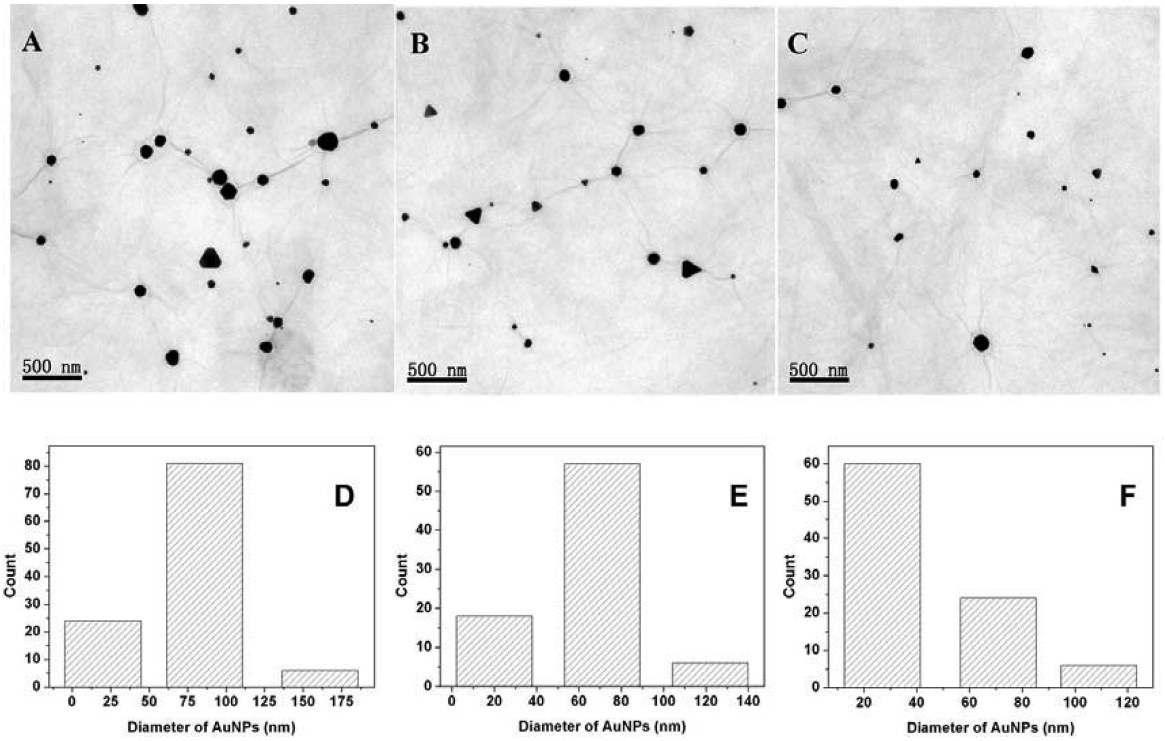

Figure 1. TEM images of G-Au NCs (upper) in different conditions and corresponding size distribution histograms of nanoparticles (below). (A, D) G-Au NCs, (B, E) G-Au NCs + $Na_2S_2O_3$, and (C, F) G-Au NCs + $Na_2S_2O_3$ + 2-ME+Pb^{2+} (100 nM).

concerns throughout the world because of their potential toxicity effects toward animals and human.[26−31] Among heavy metals, lead (Pb) is of great toxicological interest becaues of its damage to the kidney and nervous system. For these reasons, the measurement of Pb^{2+} is becoming more common and imperative in chemical, environmental, clinical and toxicology fields.[32−35] Various methods are available for the determination of Pb^{2+} in aqueous samples. For examples, Liu et al. have developed a colorimetric sensing platform based on DNAzyme-directed assembly of AuNPs for the detection of Pb^{2+}.[36] Wu et al. have demonstrated an electrochemical method for detection of Pb^{2+} on the basis of 2,5-dimercapto-1,3,4-thiadiazole self-assembled monolayer on gold electrode.[37] Saito and co-workers have reported a direct fluorescence detection of Pb^{2+} by high-performance liquid chromatography.[38]

Herein, we proposed a novel platform for effective sensing of Pb^{2+} using G-Au NCs, taking advantage of the quenching capability of AuNPs as well as the optical property of graphene. Graphene was used as fluorescence creating source, and the interaction between graphene and AuNPs could cause the fluorescence intensity to decrease/quench. Moreover, Pb^{2+} could accelerate the leaching rate of the AuNPs on the surface of graphene. Upon the addition of Pb^{2+}, the fluorescence of graphene could reappear and increase, showing "turn-on" fluorescence observation. The detection occurred with high sensitivity and selectivity toward Pb^{2+} using G-Au NCs, which was based on graphene photoluminescence quenched by AuNPs through FRET. As far as we know, this is the first application of graphene fluorescence "turn-on" to detect Pb^{2+}, and it offers an ideal alternative for sensitive detection of heavy metal ions.

EXPERIMENTAL SECTION

Chemicals and Materials. Graphene oxide was purchased from Nanjing XFNano Materials Technology Company (Nanjing, China). 2-mercaptoethanol (2-ME), sodium thiosulfate ($Na_2S_2O_3$), ethylene glycol, gold chloride trihydrate ($HAuCl_4{\cdot}3H_2O$), KCl, $MgCl_2$, $CaCl_2$, $CrCl_3$, $MnCl_2$, $FeCl_2$, $CoCl_2$, $NiCl_2$, $CuCl_2$, $ZnCl_2$, $Cd(ClO_4)_2$, $AlCl_3$, $Pb(NO_3)_2$, $HgCl_2$, and $AgNO_3$ were obtained from Sinopharm Chemical Reagent (Shanghai, China). All chemicals were of analytical grade. Buffer solution was 5 mM glycine solution (pH 10.0) and the pH was adjusted with 1.0 M NaOH. Deionized water (18.2 MΩ cm specific resistance) obtained with a Pall Cascada laboratory water system (USA) was used throughout.

Instrumentation. Transmission electron microscopy (TEM) images were captured on a JEM-1230 electron microscope operating

dx.doi.org/10.1021/am201711j | ACS Appl. Mater. Interfaces 2012, 4, 1080−1086

at 100 kV (Japan). The fluorescence spectra were recorded on a HORIBA Scientific Fluoromax-4 spectrofluorometer (France).

Synthesis of G-Au NCs. G-Au NCs were synthesized according to the procedure reported.[14] Generally, 1 mg/mL graphene oxide (10 mL) was sonicated for 1 h to form stable graphene oxide colloid. Then, 0.5 mL of 10 mM $HAuCl_4$ and 20 mL of ethylene glycol were added to the graphene oxide colloid solution with magnetic stirring for 30 min. After that, the mixture was heated to 100 °C and aged at that temperature for 6 h. Finally, the bulk samples of G-Au NCs could be obtained by centrifugation and washed with deionized water and ethanol for several times. Graphene was synthesized by the similar way without of the $HAuCl_4$.

Synthesis of AuNPs. AuNPs were synthesized by reducing $HAuCl_4$ using trisodium citrate method.[39] 100 mL of 1 mM $HAuCl_4$ was brought to a vigorous boil with stirring in a round-bottom flask fitted with a reflux condenser, and then 38.8 mM trisodium citrate (10 mL) was added rapidly to the solution, resulting in a change in solution color from pale yellow to deep red. And then the solution was boiled for another 15 min. Finally, the solution was cooled to room temperature with continuous stirring. A typical solution of 13 nm diameter gold particles exhibited a characteristic absorption at 519 nm.

Solution Preparation. For Pb^{2+} sensing, aliquots of 2700 μL of 5 mM glycine-NaOH (pH 10.0) solutions containing 100 μL of 100 ng/mL G-Au NCs, 30 μL of 100 mM $Na_2S_2O_3$, and Pb^{2+} with various concentrations (final concentration: 0−1000 nM) were equilibrated at room temperature for 15 min. Then 2-ME (10 mM, 300 μL) was added into each of these mixtures. After equilibrating through gentle shaking at room temperature for another 1.0 h, the resultant solutions were subjected to fluorescence analysis.

Water Sample Preparation. Tap water was collected after flowing for about 5 min in our laboratory when needed. Barreled mineral water, i.e., KunYu mountain mineral water, was purchased from local supermarket. For tap water samples, three aliquots of 5-fold diluted tap water were spiked with standard Pb^{2+} solutions to result in different final concentrations (50, 100, and 500 nM). For mineral water, three aliquots of 2-fold diluted KunYu mountain mineral water were spiked with standard Pb^{2+} solutions to result in different final concentrations (50, 100, and 500 nM). All the water samples with and without spiking were analyzed by the developed method.

RESULTS AND DISCUSSION

Sensing Strategy. Scheme 1 illustrates the sensing strategy for Pb^{2+} based on G-Au NCs. The G-Au NCs were synthesized by an in situ method of nucleating AuNPs in the presence of GO and ethylene glycol.[14] Subsequently, in thiosulfate liquors, AuNPs could react with thiosulfate, and complexes were formed immediately on the AuNPs surfaces. Usually the complexes were reported as $Au(S_2O_3)_2^{3-}$.[21] After adding Pb^{2+} and 2-ME, the AuNPs could rapidly be dissolved to form $Au(2\text{-}ME)_2^-$ complexes in solution. As a result, the fluorescence of the G-Au NCs increased owing to the gradual dissolution of AuNPs.

AuNPs played a pivotal role in reduction of GO with ethylene glycol, leading to the formation of G-Au NCs, as shown in Figure 1A, D (diameter of AuNPs about 86 ± 30 nm (70%)). The results demonstrated that the metal salt could not only be easily reduced in the water-ethylene glycol solution but also grow in situ on the defects originating from the oxygenation of graphite by strong oxidant.[14] The resulting graphene itself had the characteristic of photoluminescence which was dependent on the electron−hole pairs that were localized in small sp^2 carbon clusters embedded within a sp^3 matrix.[9] However, the AuNPs on the surface of graphene could quench fluorescence by FRET between graphene sheets and AuNPs. After adding $Na_2S_2O_3$ solution, the $S_2O_3^{2-}$ ions reacted with AuNPs to generate $Au(S_2O_3)_2^{3-}$ complexes owing to low-spin d^{10} Au^+ ions {log $\beta[Au(S_2O_3)_2^{3-}] \approx 26$}.[21,40] And the complexes formed a dense passive layer on the surface of AuNPs in the presence of dissolved oxygen (eq 1),[21,25] resulting in slight decrease of the size of AuNPs on the surface of graphene, as shown in Figure 1B, E (diameter about 79 ± 35 nm (70%)).

$$4Au^0 + O_2 + 2H_2O + 8S_2O_3^{2-} \rightarrow 4Au(S_2O_3)_2^{3-} + 4OH^- \quad (1)$$

And, because of a high activation energy (E_a = 27.99 kJ/mol) in the absence of a redox mediator such as Cu^+/Cu^{2+}, the leaching rate of AuNPs became lower in the system of $S_2O_3^{2-}$.[19,21,41] Fortunately, alkanethiols, such as 2-mercaptoethanol (2-ME), were strong etching agents because of the high Au−S band energy (184 kJ/mol).[25,42] The stability constant for $Au(SH)_2^-$ species {log $\beta[Au(2\text{-}ME)_2^-] \approx 30$} indicated that $Au(2\text{-}ME)_2^-$ was 4 orders of magnitude more stable than the complexes $Au(S_2O_3)_2^{3-}$ in aqueous solution at 298 K, corresponding to a free energy difference of 22.6 kJ/mol.[25,40] However, if there was only 2-ME, i.e. in the absence of $Na_2S_2O_3$, the G-Au NCs would aggregate.[25] So, we supposed that the redox mediator (RS-SR/RSH) of 2-ME involved in the thiosulfate leaching system could increase the leaching rate of the $S_2O_3^{2-}$-AuNPs. Chen and co-workers have reported that the Pb^{2+} could accelerate the dissolution of gold in the 2-ME/$S_2O_3^{2-}$-AuNPs system.[25] Pb^{2+} could react with gold to form $AuPb_2$, $AuPb_3$ alloy or metallic Pb on the surface of gold, leading to a potential drop of the gold and thus an increased rate of dissolution.[25] So, in the existence of 2-ME/$S_2O_3^{2-}$, Pb^{2+} played an important role to accelerate the leaching rate of AuNPs from the surface of graphene. As shown in Figure 1C, F, the size of AuNPs was significantly decreased (diameter $\leq$ 38 nm (70%)), which was in consistent with that reported.[25] It should be noted that, separate existence of $S_2O_3^{2-}$, 2-ME, or Pb^{2+} could not lead to fluorescence increase. Therefore, in this system, $S_2O_3^{2-}$ was primarily used as a stabilizing agent, 2-ME acted as both a reducing agent and a complexing agent, and Pb^{2+} could enable and accelerate the reaction. The developed sensing strategy for Pb^{2+} was based on the fact that Pb^{2+} could accelerate the leaching rate of AuNPs on the surface of graphene by $S_2O_3^{2-}$ and 2-ME, accompanied with fluorescence recovery and increase of graphene.

To further verify the roles that $S_2O_3^{2-}$, 2-ME, and Pb^{2+} played in accelerating the leaching rate of AuNPs, we monitored the fluorescence intensity of graphene. As seen from Figure 2, the fluorescence spectrum of G-Au NCs in 5 mM glycine-NaOH solution (pH 10.0) was displayed (curve a), and a low fluorescence emission appeared at 380 nm. In the presence of 1.0 mM $Na_2S_2O_3$ (curve b), although the size of AuNPs had a slight decrease, the fluorescence intensity of graphene was similar to that given by curve a because of the low leaching rate of AuNPs. After addition of 1.0 mM 2-ME, the fluorescence intensity of graphene increased slightly (curve *c*), which was consistent with the increased leaching rate of AuNPs. If there were only G-Au NCs and Pb^{2+}, the AuNPs could not be leached and thereby the fluorescence of graphene was still low (curve d). In the existence of AuNPs, $Na_2S_2O_3$, 2-ME, and Pb^{2+}, fluorescence was hardly observed (curve e), indicating that the fluorescence was almost completely from the graphene, and only a slight interference was caused by the AuNPs, $Na_2S_2O_3$, 2-ME, and Pb^{2+}. With the assistance of 2-ME/$Na_2S_2O_3$ and Pb^{2+}, the AuNPs would be acceleratedly oxidized and leached into the solution, and thereby

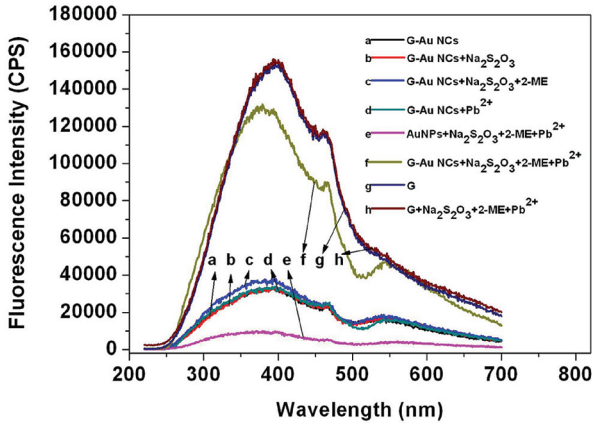

Figure 2. Fluorescence spectra of G-AuNCs at different conditions: (a) G-AuNCs (3 ng/mL) in glycine-NaOH buffer (black line); (b) G-AuNCs (3 ng/mL) + $Na_2S_2O_3$ (1.0 mM); (c) G-AuNCs (3 ng/mL) + $Na_2S_2O_3$ (1.0 mM)+2-ME(1.0 mM); (d) G-AuNCs (3 ng/mL) + Pb^{2+} (1000 nM); (e) AuNPs (5 μL) + $Na_2S_2O_3$ (1.0 mM) + 2-ME (1.0 mM) + Pb^{2+} (1000 nM); (f) G-AuNCs (3 ng/mL) + $Na_2S_2O_3$ (1.0 mM) + 2-ME (1.0 mM)+Pb^{2+} (500 nM); (g) G (3 ng/mL); h) G (3 ng/mL) + $Na_2S_2O_3$ (1.0 mM) + 2-ME (1.0 mM)+Pb^{2+} (1000 nM).

fluorescence intensity of graphene was dramatically increased as shown in curve f of Figure 2. At the same time, according to curves g and h, it could be concluded that the fluorescence of graphene could be quenched only by AuNPs. Therefore, in this system, the sensing mechanism for Pb^{2+} was based on the accelerated leaching effect of AuNPs on the graphene surfaces in the presence of both $S_2O_3^{2-}$ and 2-ME.

Parameter Optimization. Sensitivity of the fluorescence detection strongly depended on the main experimental parameters including size of GO, concentration of $HAuCl_4$, pH, concentration of $Na_2S_2O_3$, concentration of 2-ME and reaction time. The effects of these parameters had been systematically investigated as follows.

Effect of GO Size and $HAuCl_4$ Concentration. The fluorescence properties of graphene was strongly dependent on the size of the precursors GO. When the length or width of GO was >1 μm, the fluorescence "turn-on" efficiency was low, resulting in low sensitivity of fluorescence detection. So in our system, the size of GO <1 μm was used.

The fluorescence "turn-on" efficiency was influenced by the total amount of AuNPs on the surface of graphene, which was determined by the concentration of $HAuCl_4$. The relationship between the concentration of $HAuCl_4$ and the relative fluorescence intensity was investigated and the corresponding results were shown in Figure 3A, where F_0 and F were fluorescence intensities at 380 nm in the absence and presence of Pb^{2+} ions (1.0 μM), respectively. It could be seen that the relative fluorescence intensity gradually increased in the concentration range of 0.2−1.0 mM, which was because of the increased amount of AuNPs that would increase the fluorescence quenching efficiency of AuNPs to graphene. At concentration >1.0 mM, the relative fluorescence intensity of graphene decreased, which was probably due to the fact that AuNPs on the surface of graphene were close to saturation and the superabundant AuNPs in the solution reacted with Pb^{2+}, and thereby decreased quenching efficiency of AuNPs to graphene. Therefore, the optimal concentration of $HAuCl_4$ was chosen as 1.0 mM.

Effect of pH. The pH of the solution would affect the leaching of AuNPs in the 2-ME/$S_2O_3^{2-}$−G-Au NCs system in the absence and presence of Pb^{2+} ions. Therefore, it was

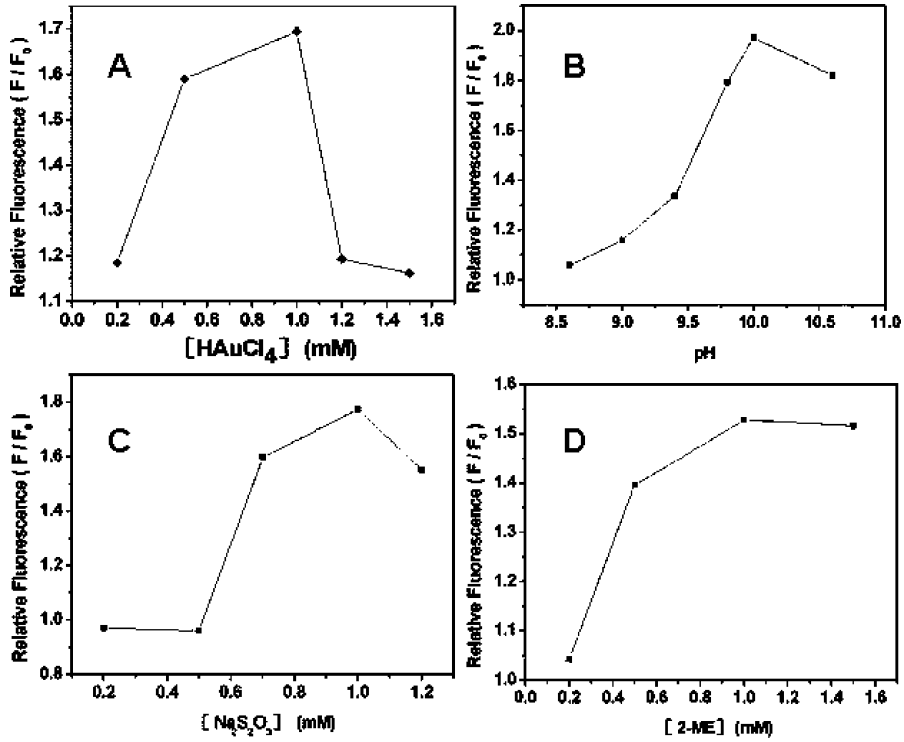

Figure 3. Effects of (A) concentration of $HAuCl_4$ (0.2−1.5 mM), (B) pH (8.6−10.6), (C) concentration of $Na_2S_2O_3$ (0.2−1.2 mM) and (D) concentration of 2-ME (0.2−1.5 mM) on the relative fluorescence intensity changes of graphene. The concentration of Pb^{2+} was 1000 nM and excitation was 200 nm.

dx.doi.org/10.1021/am201711j | ACS Appl. Mater. Interfaces 2012, 4, 1080−1086

necessary to investigate the effect of pH on the fluorescence response. Figure 3B shows the relative fluorescence intensity of graphene in various pH solutions. When the pH shifted from 8.6 to 10.0, the relative fluorescence intensity of graphene increased greatly, which was attributed to two aspects: (i) $S_2O_3^{2-}$ was more stable in the solution at higher pH and (ii) $Au(2\text{-ME})_2^-$ complexes were more stable at pH greater than the pK_a (8.8–9.1) of 2-ME.[43,44] However, further increasing the pH could cause a relatively lower fluorescence intensity, which might be mainly because of the formation of passive layers of $Pb(OH)_2$, PbO, $Au(OH)_3$, or Au_2O_3 on the surface of the AuNPs.[25] So, pH 10.0 was selected as the optimal pH value.

Effect of $Na_2S_2O_3$ Concentration. $Na_2S_2O_3$ had been demonstrated to act as both a reducing and a stabilizing agent for the dissolution of gold. The reduction ability of $Na_2S_2O_3$ was subsidiary, and the stabilizing power was primary. From Figure 3C, we could observe that the relative fluorescence intensity of graphene increased with the increased concentration of $Na_2S_2O_3$ in the range of 0.2–1.0 mM. The increased response might result from the increase of stability. Further increasing the concentration of $Na_2S_2O_3$ would induce a relative lower response. That was because the increased thickness of the passive layer hindered Pb^{2+} and 2-ME to contact the surface of AuNPs and therefore decreased the leaching rate. Thus, 1.0 mM $Na_2S_2O_3$ was used in the following work.

Effect of 2-ME Concentration. Figure 3D shows the effect of the 2-ME concentration (0.2–1.5 mM) on the relative fluorescence intensity of graphene in the absence and presence of Pb^{2+} ions (1.0 μM). Here, 2-ME acted as both a reducing agent and a complexing agent. Obviously, lower concentrations of 2-ME in the solution yielded smaller relative fluorescence intensity of graphene; and an increase in the concentration of 2-ME yielded greater relative fluorescence intensity. This might be ascribed to the increased dissolution rate of AuNPs into the solution. The response to 1.0 μM Pb^{2+} increased rapidly with the concentration of 2-ME increase until 1.0 mM, and then tended to increase slowly. So, 1.0 mM 2-ME was used in this work.

Effect of Reaction Time. The sensitivity of the proposed method for detection of Pb^{2+} was undoubtedly promoted with the increase of the reaction time because of the increased leaching amount of AuNPs into the solution. However, this tendency would not be prolonged all the time. As shown in Figure 4, the response to 100 nM Pb^{2+} increased rapidly with the reaction time increasing up to 40 min, and then began to level off. To obtain stable fluorescence, 1.0 h was chosen as the reaction time.

Sensitivity and Selectivity. Under the above optimized conditions, the method performance was evaluated for the determination of Pb^{2+}. As shown in Figure 5, the intensity of the fluorescence emission of graphene increased upon increasing the concentration of Pb^{2+}. The graphene showed a good linear response of the relative fluorescence intensity with respect to the logarithm of the Pb^{2+} concentration in the range of 50–1000 nM (R = 0.9982) as shown in the inset. The error bars (relative standard deviation (RSD), less than 0.3%) of the relative fluorescence intensity were relatively small, indicating that the method is quite stable and reproducible. The minimum detectable concentration using the method was obtained of 10 nM, which was lower than the maximum contamination level (MCL) of 72 nM for Pb^{2+} in drinking water as defined by the U.S. Environmental Protection Agency (EPA).[45] A number of

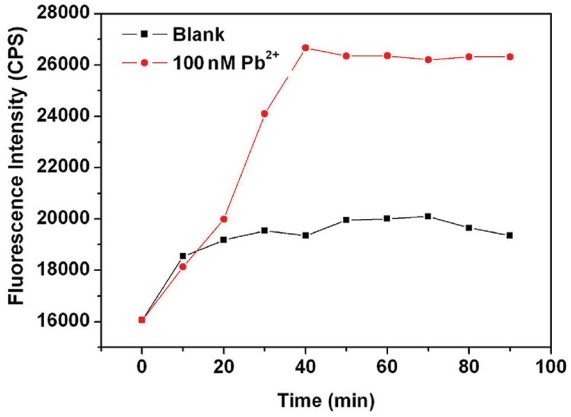

Figure 4. Effect of time on the fluorescence intensity of graphene without and with the presence of 100 nM Pb^{2+}. Excitation: 200 nm.

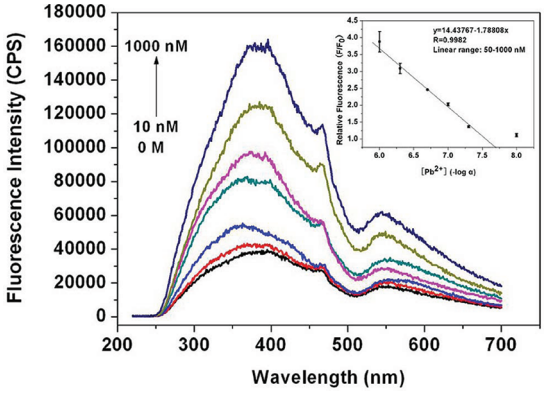

Figure 5. Fluorescence spectra of G-Au NCs in 5 mM glycine solution upon the addition of increasing concentrations of Pb^{2+} ions (0 M–1000 nM) under the optimal conditions. The inset was the calibration curve of the G-Au NCs for detection of Pb^{2+} ions. Error bars were obtained from five parallel experiments.

studies for the detection of Pb^{2+} have been reported, so some methods based on AuNPs were summarized and compared with the present work, as listed in Table 1. As can be seen from the table, as a new sensing strategy, the "turn-on" fluorometry based on accelerated leaching of AuNPs on the surface of graphene is an ideal candidate for sensitive detection of Pb^{2+} ions.

To further verify the performance of the developed method for Pb^{2+} in practical applications, we investigated the selectivity of this turn-on fluorescence response toward Pb^{2+} ions. Other metal ions commonly found coexistent with Pb^{2+}, including Al^{3+}, Ca^{2+}, Cd^{2+}, K^+, Mg^{2+}, Zn^{2+}, Li^+, Co^{2+}, Ni^{2+}, Hg^{2+}, Cu^{2+}, Ag^+, Mn^{2+}, Cr^{3+}, and Fe^{2+}, were tested. The relative fluorescence intensity of the solution containing 1.0 μM Pb^{2+} and other metal ions individual, respectively, were shown in Figure 6. The results showed that 100-fold of Al^{3+}, Ca^{2+}, Cd^{2+}, K^+, Mg^{2+}, Zn^{2+}, Li^+, Co^{2+}, and Ni^{2+}, 10-fold of Hg^{2+}, Cu^{2+}, Ag^+, and Mn^{2+}, and 5-fold of Cr^{3+} and Fe^{2+} had much lower fluorescence intensity than that of 1.0 μM Pb^{2+}. The developed method supplied an attractive selectivity for Pb^{2+}.

Practical Application. To evaluate the practicality of the developed sensing platform, we further carried out the recovery experiments by analyzing the tap water and mineral water samples. No Pb^{2+} was detected in the tap water and mineral water. Then, standard addition technique was used. Three

Table 1. Comparison of Linear Range and Limit of Detection (LOD) for Detection of Pb^{2+} Using AuNP-Based Methods

detection techniques	recognition probe	assisted probe	linear range	LOD	ref
fluorometry		G-Au NCs	50−1000 nM	10 nM	this work
fluorometry	cysteamine and 11-mercaptoundecanoic acid	CdTe-QDs and AuNPs	0.22−4.51 ppm	30 ppb	46
colorimetry	DNAzymes	AuNPs	0.4−2 μM	0.4 μM	47
colorimetry	DNAzyme	AuNPs	100 nM−4 μM	100 nM	36
colorimetry	gallic acid	AuNPs	10−1000 nM	10 nM	48
colorimetry	DNAzyme	AuNPs	3 nM−1 μM	3 nM	49
colorimetry		AuNPs	2.5 nM−10 μM	0.5 nM	25
mass spectrometry		AuNPs	1.0×10^{-9}−5.0×10^{-6} M	0.5 nM	50

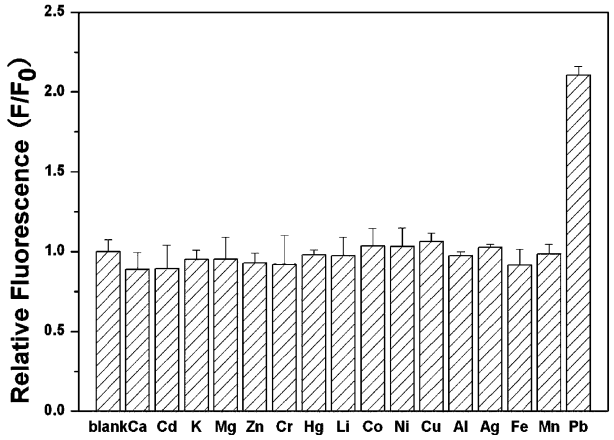

Figure 6. Relative fluorescence responses of G-Au NCs in 5 mM glycine solution upon the addition of various metal ions. The concentration of Al^{3+}, Ca^{2+}, Cd^{2+}, K^{+}, Mg^{2+}, Zn^{2+}, Li^{+}, Co^{2+}, and Ni^{2+} was 100 μM, respectively, the concentration of Hg^{2+}, Cu^{2+}, Ag^{+}, Mn^{2+} was 10 μM, respectively, and the concentration of Cr^{3+}, Fe^{2+} was 5 μM, respectively; the concentration of Pb^{2+} was 1.0 μM.

levels of 50, 100, and 500 nM Pb^{2+} were spiked to 5-fold diluted tap water and 2-fold diluted mineral water samples, respectively. Five replicate analyses were performed for each sample to determine recoveries and the measured results of the water samples were listed in Table 2. Satisfactory recoveries of

Table 2. Recoveries for the Detection of Pb^{2+} in Water Samples (n = 5)

samples	added (nM)	recovery (%)	RSD (%)
tap water	50	91.4	1.30
	100	102.0	1.08
	500	90.6	1.21
mineral water	50	104.4	0.91
	100	110.8	6.92
	500	92.1	8.08

Pb^{2+} were obtained, namely, 90.6−102.0% with the precision of 1.08−1.30% for tap water, and 92.1−110.8% with the precision of 0.91−8.08% for mineral water, respectively. This demonstrated the developed method potentially applicable for the detection of Pb^{2+} in water samples.

CONCLUSIONS

In summary, a novel "turn-on" fluorescent chemosensor was developed for Pb^{2+} by using G-Au NCs, based on the accelerated leaching of AuNPs on graphene surfaces that induced the restoration and enhancement of graphene fluorescence. In particular, this assay allowed selective detection of Pb^{2+} as low as 10 nM in aqueous solution using a very simple approach. Moreover, the method provided potential opportunities for sensitive detection of heavy metal ions by virtue of the analyte-induced depletion of quenchers. Thus the development of new strategies based on similar reactions has a promising future in environmental analysis/monitoring and other related fields.

AUTHOR INFORMATION

Corresponding Author

*E-mail: lxchen@yic.ac.cn.

Notes

The authors declare no competing financial interest.

ACKNOWLEDGMENTS

Financial support from the National Natural Science Foundation of China (20975089), the Innovation Projects of the Chinese Academy of Sciences (KZCX2-EW-206), the Department of Science and Technology of Shandong Province (BS2009DX006), the Department of Science and Technology of Yantai City of China (2007156, 2011426) and the 100 Talents Program of the Chinese Academy of Sciences is gratefully acknowledged.

REFERENCES

(1) Geim, A. K.; Novoselov, K. S. *Nat. Mater.* **2007**, *6*, 183−191.
(2) Jiao, L. Y.; Zhang, L.; Wang, X. R.; Diankov, G.; Dai, H. J. *Nature* **2009**, *458*, 877−880.
(3) Geim, A. K. *Science* **2009**, *324*, 1530−1534.
(4) Goh, M. S.; Pumera, M. *Anal. Bioanal. Chem.* **2011**, *399*, 127−131.
(5) Varghese, N.; Mogera, U.; Govindaraj, A.; Das, A.; Maiti, P. K.; Sood, A. K.; Rao, C. N. R. *Chem. Phys. Chem.* **2009**, *10*, 206−210.
(6) Liu, Z.; Robinson, J. T.; Sun, X. M.; Dai, H. J. *J. Am. Chem. Soc.* **2008**, *130*, 10876−10877.
(7) Lu, C. H.; Yang, H. H.; Zhu, C. L.; Chen, X.; Chen, G. N. *Angew. Chem., Int. Ed.* **2009**, *48*, 4785−4787.
(8) Wen, Y. Q.; Xing, F. F.; He, S. J.; Song, S. P.; Wang, L. H.; Long, Y. T.; Li, D.; Fan, C. H. *Chem. Commun.* **2010**, *46*, 2596−2598.
(9) Eda, G.; Lin, Y. Y.; Mattevi, C.; Yamaguchi, H.; Chen, H. A.; Chen, I. S.; Chen, C. W.; Chhowalla, M. *Adv. Mater.* **2010**, *22*, 505−509.
(10) Subrahmanyam, K. S.; Kumar, P.; Nag, A.; Rao, C. N. R. *Solid State Commun.* **2010**, *150*, 1774−1777.
(11) Loh, K. P.; Bao, Q.; Eda, G.; Chhowalla, M. *Nat. Chem.* **2010**, *2*, 1015−1024.
(12) Jung, J. H.; Cheon, D. S.; Liu, F.; Lee, K. B.; Seo, T. S. *Angew. Chem., Int. Ed.* **2010**, *49*, 5708−5711.
(13) Liu, F.; Choi, J. Y.; Seo, T. S. *Biosens. Bioelectron.* **2010**, *25*, 2361−2365.
(14) Xu, C.; Wang, X.; Zhu, J. W. *J. Phys. Chem., C* **2008**, *112*, 19841−19845.

(15) Fu, X. Q.; Bei, F. L.; Wang, X.; O'Brien, S.; Lombardi, J. R. *Nanoscale* **2010**, *2*, 1461−1466.
(16) Li, D.; Müller, M. B.; Gilje, S.; Kaner, R. B.; Wallace, G. G. *Nat. Nanotechnol.* **2008**, *3*, 101−105.
(17) Dubertret, B.; Calame, M.; Libchaber, A. J. *Nat. Biotechnol.* **2001**, *19*, 365−370.
(18) Pons, T.; Medintz, I. L.; Sapsford, K. E.; Higashiya, S.; Grimes, A. F.; English, D. S.; Mattoussi, H. *Nano Lett.* **2007**, *7*, 3157−3164.
(19) Feng, D.; Van Deventer, J. S. J. *Hydrometallurgy* **2002**, *64*, 231−246.
(20) Senanayake, G. *Miner. Eng.* **2004**, *17*, 785−801.
(21) Grosse, A. C.; Dicinoski, G. W.; Shaw, M. J.; Haddad, P. R. *Hydrometallurgy* **2003**, *69*, 1−21.
(22) Senanayake, G. *Hydrometallurgy* **2008**, *90*, 46−73.
(23) Sandenbergh, R. F.; Miller, J. D. *Miner. Eng.* **2001**, *14*, 1379−1386.
(24) McIntyre, J. D. E. Jr.; W., F. P. *J. Electrochem. Soc.* **1976**, *123*, 1800−1813.
(25) Chen, Y. Y.; Chang, H. T.; Shiang, Y. C.; Hung, Y. L.; Chiang, C. K.; Huang, C. C. *Anal. Chem.* **2009**, *81*, 9433−9439.
(26) Järup, L. *Brit. Med. Bull.* **2003**, *68*, 167−182.
(27) Hayes, R. B. *Cancer Cause Control* **1997**, *8*, 371−385.
(28) Lou, T. T.; Chen, Z. P.; Wang, Y. Q.; Chen, L. X. *ACS Appl. Mater. Interfaces* **2011**, *3*, 1568−1573.
(29) Li, J. L.; Chen, L. X.; Lou, T. T.; Wang, Y. Q. *ACS Appl. Mater. Interfaces* **2011**, *3*, 3936−3941.
(30) Lou, T. T.; Chen, L. X.; Chen, Z. P.; Wang, Y. Q.; Chen, L.; Li, J. H. *ACS Appl. Mater. Interfaces* **2011**, *3*, 4215−4220.
(31) Wang, G. Q.; Chen, Z. P.; Wang, W. H.; Yan, B.; Chen, L. X. *Analyst* **2011**, *136*, 174−178.
(32) Yantasee, W.; Timchalk, C.; Lin, Y. H. *Anal. Bioanal. Chem.* **2007**, *387*, 335−341.
(33) Knecht, M. R.; Sethi, M. *Anal. Bioanal. Chem.* **2009**, *394*, 33−46.
(34) Zhang, N.; Peng, H. Y.; Wang, S.; Hu, B. *Microchim. Acta* **2011**, *175*, 121−128.
(35) Pauget, B.; Gimbert, F.; Coeurdassier, M.; Scheifler, R.; Vaufleury, A. *J. Hazard. Mater.* **2011**, *192*, 1804−1811.
(36) Liu, J. W.; Lu, Y. *J. Am. Chem. Soc.* **2003**, *125*, 6642−6643.
(37) Wu, Y.; Li, N. B.; Luo, H. Q. *Microchim. Acta* **2008**, *160*, 185−190.
(38) Saito, S.; Danzaka, N.; Hoshi, S. *J. Chromatogr., A* **2006**, *1104*, 140−144.
(39) Frens, G. *Nat. Phys. Sci.* **1973**, *241*, 20−22.
(40) Bryce, R. A.; Charnock, J. M.; Pattrick, R. A. D.; Lennie, A. R. *J. Phys. Chem., A* **2003**, *107*, 2516−2523.
(41) Senanayake, G. *Gold Bull.* **2005**, *38*, 170−179.
(42) Dubois, L. H.; Nuzzo, R. G. *Annu. Rev. Phys. Chem.* **1992**, *43*, 437−463.
(43) Renders, P. J.; Seward, T. M. *Geochim. Cosmochim. Acta* **1989**, *53*, 245−253.
(44) Pyykkö, P. *Inorg. Chim. Acta* **2005**, *358*, 4113−4130.
(45) http://www.epa.gov/safewater/contaminants/index.html (accessed June 2008).
(46) Wang, X.; Guo, X. Q. *Analyst* **2009**, *134*, 1348−1354.
(47) Liu, J. W.; Lu, Y. *J. Am. Chem. Soc.* **2004**, *126*, 12298−12305.
(48) Huang, K. W.; Yu, C. J.; Tseng, W. L. *Biosens. Bioelectron.* **2010**, *25*, 984−989.
(49) Wang, Z. D.; Lee, J. H.; Lu, Y. *Adv. Mater.* **2008**, *20*, 3263−3267.
(50) Liu, Y. C.; Chiang, C. K.; Chang, H. T.; Lee, Y. F.; Huang, C. C. *Adv. Funct. Mater.* **2011**, *21*, 4448−4455.